Propagating and evanescent modes in two-dimensional wire media

I. S. Nefedov,[1,*] A. J. Viitanen,[2,†] and S. A. Tretyakov[1,‡]
[1]*Radio Laboratory/SMARAD, Department of Electrical and Communications Engineering, Helsinki University of Technology (TKK), P. O. Box 3000, FI-02015 TKK, Finland*
[2]*Electromagnetics Laboratory, Department of Electrical and Communications Engineering, Helsinki University of Technology (TKK), P. O. Box. 3000, FI-02015 TKK, Finland*
(Received 16 December 2004; published 29 April 2005)

Electromagnetic waves in an artificial medium formed by two mutually orthogonal lattices of thin ideally conducting straight wires (referred to as a two-dimensional wire medium) are considered. An effective medium approach and a full-wave method based on the dyadic Green's function and the method of moments are developed. Effects of spatial dispersion, such as the appearance of anisotropy in a square lattice and an additional extraordinary wave, as in crystal optics, are demonstrated. Evanescent waves with complex propagation constants are found. The case when both forward and backward extraordinary waves with respect to an interface exist simultaneously is observed and discussed. The effect of birefringence, so that one extraordinary wave has the wave vector making a positive angle to the interface and the other has the wave vector making a negative angle to the interface, is illustrated.

DOI: 10.1103/PhysRevE.71.046612 PACS number(s): 41.20.Jb, 42.70.Qs, 77.22.Ch, 77.84.Lf

I. INTRODUCTION

The wire medium (a medium formed by a lattice of ideally conducting parallel thin wires) has been known for a long time [1]. Such a medium is usually described at low frequencies as a uniaxial material, whose relative permittivity dyadic can be written as (the wires are in the z direction)

$$\bar{\bar{\epsilon}} = \epsilon_h(\mathbf{u}_x\mathbf{u}_x + \mathbf{u}_y\mathbf{u}_y) + \epsilon_z\mathbf{u}_z\mathbf{u}_z, \tag{1}$$

where ϵ_z is expressed by the plasma formula

$$\epsilon_z = \epsilon_h\left(1 - \frac{\omega_p^2}{\omega^2\epsilon_h}\right) = \epsilon_h\left(1 - \frac{k_p^2}{k^2}\right). \tag{2}$$

Here ϵ_h is the permittivity of the host medium, $k=\omega/c\sqrt{\epsilon_h} = k_0\sqrt{\epsilon_h}$, and c is the speed of light. The constant ω_p (or the corresponding k_p) is an equivalent "plasma frequency" that gives grounds to call the wire medium an "artificial plasma." There exist different models for the plasma frequency, and we will use below the formula for k_p obtained in [2]. However, it has been shown that if the wave vector in a wire medium (WM) has a nonzero component along the wires, the plasma model (2) gives nonphysical results [3]. The plasma model has been corrected by introducing spatial dispersion (SD) into formula (2). A detailed study of wave propagation in an arbitrary tilted wire medium slab, taking into account SD, was performed in [4].

Not only arrays of wires along one direction have been studied before. An artificial structure, composed of infinite wires arranged in a cubic lattice, joined at the corners of the lattice, was considered in [5]. Such a medium is expected to behave as an isotropic electromagnetic crystal with a negative permittivity at low frequencies given by formula (2). This model does not take into account spatial dispersion which may be expected there in analogy with the one-dimensional (1D) case. Also at the same time a 3D wire mesh grid with covalently bonded diamond structure was studied in [6]. Both connected and disconnected 3D lattices have been studied in [7], where the presence of spatial dispersion in a 3D WM was demonstrated numerically for propagating modes near the plasma resonance. For certain propagation directions, the results of [7] can be directly applied to the present problem of two-set lattices, and whenever possible, we compare our results with [7]. Finally, a 2D WM was considered in [8] using a semianalytical method based on the local field approach. The present effective medium and numerical methods significantly complement the local field approach proposed in [8].

Much more interest in wire media appeared at the end of the last decade in connection with engineering of materials with negative parameters, sometimes called *double negative materials* (DNMs). The first DNM proposed by Smith *et al.* consists of a lattice of long metal strips and split-ring resonators [9]. Now the wire medium is a commonly used component of artificial metamaterials for microwave and optical applications [10].

In this paper we consider an artificial medium formed of two mutually perpendicular nonconnected wire arrays (see Fig. 1). We assume that the wire arrays are identical, the period of the lattice is equal to L in the x, y, and z directions, and the radius of the wires is equal to r_0. In this case the wire lattice is square in the plane of the wires, i.e., the (yz) plane. We assume that the wires are thin and take into account only longitudinal currents. In the framework of the conventional model it would be reasonable to suppose that such a medium can be considered as a uniaxial crystal described by the permittivity dyadic (assuming that the x direction is perpendicular to the wires)

*Electronic address: igor.nefedov@tkk.fi
†Electronic address: ari.viitanen@tkk.fi
‡Electronic address: sergei.tretyakov@tkk.fi

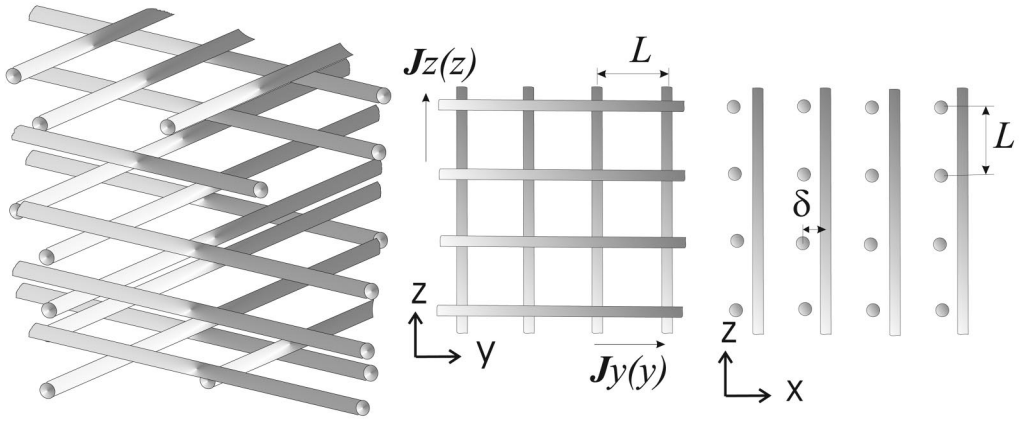

FIG. 1. Geometry of the problem.

$$\bar{\bar{\epsilon}} = \epsilon_h \mathbf{u}_x \mathbf{u}_x + \epsilon_t (\mathbf{u}_y \mathbf{u}_y + \mathbf{u}_z \mathbf{u}_z), \tag{3}$$

where ϵ_t is expressed by the plasma formula (2). Note that for the waves whose electric field vector lies in the plane of the wires (interacting with the wires) such a medium does not differ from a 3D artificial plasma formed by nonconnected wires.

Let us show that this model of the 2D WM is inconsistent, if the wave vector has components directed along the wires, similarly to the case of the usual 1D WM. Consider a rectangular waveguide, infinite along the x axis, with the cross section $a \times b$, where a and b are the sizes along the y and z axes, respectively. The waveguide propagation constant for the TM modes in a waveguide filled with a uniaxial crystal is expressed by the formula

$$k_x = \sqrt{\epsilon_t [k_0^2 - (k_y^2 + k_z^2)/\epsilon_h]}, \tag{4}$$

where $k_y = m\pi/a$, $k_z = n\pi/b$, and m and n are integers. (We assume the relative permeability of all considered media equal to unity.) Let that uniaxial crystal be a 2D WM and both of the wire arrays be perpendicular to the x axis. We obtain a preposterous result: The lower the frequency, the larger is the number of modes that propagate in the waveguide, since $\epsilon_t < 0$ at low frequencies. Thus we come of necessity to use the same model, taking into account spatial dispersion, as for the 1D wire medium [3]. A simple plasma model, generalizing the 1D case [3], was proposed in [11].

The artificial wire medium has features that are not found in any known natural media. First, the wires can be made very long in comparison with the wavelength. That is why SD is observed here at very low frequencies in contrast with other media, where SD appears when the wavelength of electromagnetic (excitonic, exchange spin, etc.) waves becomes comparable with the lattice constant. Moreover, very important for us is a class of evanescent modes that we consider in the problems of reflection from the WM, wave tunneling through a thin slab of a WM, or the waveguide problem, where the WM introduces specific boundary conditions for the medium supporting the wave propagation.

In this paper we study in detail the eigenvalue problem in a 2D WM. To solve this problem we use the effective medium (EM) approach and a numerical model, based on the dyadic Green's function method. In contrast to [8], where only some types of propagating modes were considered, we pay the main attention to evanescent modes. Knowledge of evanescent modes is especially important for applications of a 2D WM as an artificial plasma at low frequencies. We show that spatial dispersion causes the presence of waves with complex propagation constants in 2D WMs. For thin wires the results given by the EM and electrodynamical theories are in very good agreement.

II. EFFECTIVE MEDIUM THEORY AND EIGENWAVES IN AN UNBOUNDED 2D WM

In the effective medium approach the 2D wire medium is considered as a homogeneous anisotropic medium with spatial dispersion. For considering a 2D wire medium let us take a case where the wires are along the y and z directions. We consider waves in unbounded space filled with a 2D wire medium, assuming the space-time dependence of fields as $e^{i(\omega t - k_x x - k_y y - k_z z)}$. Because of spatial dispersion the crystal is anisotropic even in the yz plane, although the cell is square, i.e., the 2D WM is a biaxial crystal with the permittivity dyadic

$$\bar{\bar{\epsilon}} = \epsilon_h \mathbf{u}_x \mathbf{u}_x + \epsilon_y \mathbf{u}_y \mathbf{u}_y + \epsilon_z \mathbf{u}_z \mathbf{u}_z, \tag{5}$$

where [3,7,8,10,11]

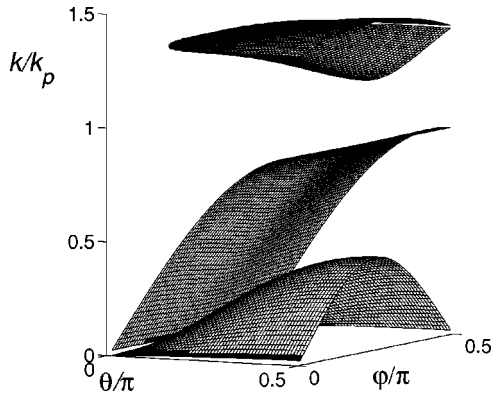

FIG. 2. Surface of the normalized frequency k/k_p versus the angles θ and φ calculated for $qL = 0.4\pi$ and $k_p L = 1.38$.

$$\epsilon_y = \epsilon_h\left(1 - \frac{k_p^2}{k_0^2\epsilon_h - k_y^2}\right), \quad \epsilon_z = \epsilon_h\left(1 - \frac{k_p^2}{k_0^2\epsilon_h - k_z^2}\right). \tag{6}$$

Note that the model (6) works for both real and imaginary k_y and k_z (evanescent waves) (see [3]). It is important that such a 2D WM is a unique "material" among other media exhibiting spatial dispersion, and we do not know any similar natural materials.

Considering an arbitrary direction of wave propagation in space, the wave vector is $\mathbf{k}=k_x\mathbf{u}_x+k_y\mathbf{u}_y+k_z\mathbf{u}_z$. Substituting the expressions for the permittivity dyadic (5) and (6) into the Maxwell equations, we come to the following eigenvalue equation:

$$\det = \begin{vmatrix} k^2 - k_y^2 - k_z^2 & k_x k_y & k_x k_z \\ k_x k_y & k^2\left(1 - \frac{k_p^2}{k^2 - k_y^2}\right) - k_x^2 - k_z^2 & k_y k_z \\ k_x k_z & k_y k_z & k^2\left(1 - \frac{k_p^2}{k^2 - k_z^2}\right) - k_x^2 - k_y^2 \end{vmatrix} = 0. \tag{7}$$

Determinant (7) results in a fourth order equation for k^2 for a fixed set k_x, k_y, and k_z. Let us denote $k_x=q\cos\theta$, $k_y=q\sin\theta\cos\varphi$, $k_z=q\sin\theta\sin\varphi$. This way we parametrize the $\mathbf{k}$ space by the number q and the angles θ and φ. The surface of the normalized frequency k/k_p versus θ and φ consists of separate branches corresponding to different propagating modes or passbands as illustrated in Fig. 2. The lowest and two higher order modes are extraordinary modes when $\theta=\pi/2$. The second mode is an ordinary one, $k=q$, and the propagation does not depend on φ at $\theta=\pi/2$. It forms the second passband when $k_x\neq 0$. Both the first and the second modes cannot propagate in the x direction, i.e., at $\theta=0$, when the electric field vector lies in the plane of the wires. Also the first and the second modes cannot propagate at any θ if $\varphi=0$ or $\pi/2$, where the vector of the electric field is parallel to the wires of one of the lattices. In these special cases the eigenvalue equation reduces to $k^2=k_x^2+k_y^2+k_p^2$ (propagation in the xy plane) and $k^2=k_x^2+k_z^2+k_p^2$ (propagation in the xz plane), respectively. The third and the fourth passbands lie in the region above the plasma resonance and are presented by surfaces, merged at $\varphi=0$ and $\pi/2$ for identical wire arrays (having the same plasma frequencies).

Let us consider in more detail one interesting special case, namely, propagation in the yz plane. The wave vector is $\mathbf{k}=k_y\mathbf{u}_y+k_z\mathbf{u}_z$, and the determinant equation (7) splits into two parts. This is also found when inserting the permittivity dyadic in the Maxwell equations: We can separate them into two subsystems, describing ordinary and extraordinary waves. For the ordinary waves, the equations are

$$-k_z H_y + \frac{k_0^2\epsilon_h - k_y^2}{k_0\eta}E_x = 0,$$

$$k_z E_x - k_0\eta H_y = 0 \tag{8}$$

(denoting η as the free space wave impedance) which results in the propagation factor for the ordinary wave: $k_z^2=k^2-k_y^2$. There are no effects due to wires for ordinary waves.

Assuming $k_z\neq 0$ for the fields of extraordinary waves, which is the most interesting case, for unbounded 2D wire media the following equations are obtained:

$$k_z E_y + \frac{k_0^2\epsilon_z - k_y^2}{k_0\epsilon_z}\eta H_x = 0,$$

$$k_z H_x + \frac{k_0\epsilon_y}{\eta}E_y = 0. \tag{9}$$

Using the effective medium model, we have the permittivities (5) and (6). In general, the plasma numbers k_p may be different due to different dimensions and placements of wires in the y and z directions. Here, for simplicity, we assume the same plasma numbers in the y and z directions. After evaluating the dispersion relation, we have a cubic equation for k^2:

$$k^6 - 2(k_y^2 + k_z^2 + k_p^2)k^4 + [(k_y^2 + k_z^2 + k_p^2)^2 + k_y^2 k_z^2]k^2 - k_y^2 k_z^2(k_y^2 + k_z^2 + 2k_p^2) = 0. \tag{10}$$

Assuming $k_y\neq 0$ we can obtain for the extraordinary wave instead of Eq. (9) a system of equations relating unknowns E_z and H_x, which results in the same equation (10).

Solving the cubic equation (10) leads to three different solutions, indicating three existing eigenwaves. Two of the eigenwaves exist near the plasma resonance and the third one in the low frequency range. The propagating and evanescent eigenwaves are studied in detail in Sec. IV. The propagation factor in the z direction is obtained from Eq. (10). Solutions for k_z^2 have the form

$$k_{z1,2}^2 = \frac{2k^4 - 2k^2k_p^2 - 3k^2k_y^2 + 2k_p^2k_y^2 + k_y^4 \mp k_y\sqrt{(k_y^2 - k^2)[(2k_p^2 + k_y^2)^2 - k^2(4k_p^2 + k_y^2)]}}{2(k^2 - k_y^2)}. \tag{11}$$

Thus, there exist four solutions for k_z, which are, in general, complex numbers describing evanescent or propagating waves in the z direction. The properties of the solutions of Eq. (11) are considered in detail in Sec. IV in comparison with numerical results obtained by the method described in the next section.

III. INTEGRAL EQUATION AND DYADIC GREEN'S FUNCTION

In this section we introduce an alternative approach (numerical method) to find eigenwaves in a periodic 2D wire medium. We use the following representation of electric field induced by currents on the wires:

$$\mathbf{E}(\mathbf{r}) = \frac{\eta}{ik_0\epsilon_h}\int_S \bar{\bar{G}}(\mathbf{r},\mathbf{r}')\mathbf{J}(\mathbf{r}')dS, \tag{12}$$

where S is the surface of the perfectly conducting metal wires on one period and the dyadic Green's function has the form

$$\bar{\bar{G}}(\mathbf{r},\mathbf{r}') = (\boldsymbol{\nabla}\,\boldsymbol{\nabla} + k_0^2\epsilon_h\bar{\bar{I}})G(\mathbf{r},\mathbf{r}'). \tag{13}$$

The scalar Green's function for 3D periodic media is expressed as

$$G(x,y,z|x',y',z') = -\frac{1}{L^3}\sum_{m=-\infty}^{\infty}\sum_{n=-\infty}^{\infty}\sum_{l=-\infty}^{\infty}\frac{e^{-i[\alpha_m\overline{x}+\beta_n\overline{y}+\gamma_l\overline{z}]}}{g_{mnl}}, \tag{14}$$

where we have denoted $\overline{x}=x-x'$, $\overline{y}=y-y'$, $\overline{z}=z-z'$, $\alpha_m=k_x+q_m$, $\beta_n=k_y+q_n$, $\gamma_l=k_z+q_l$, $q_s=2\pi s/L$, and $g_{mnl}=k_0^2\epsilon_h-\alpha_m^2-\beta_n^2-\gamma_l^2$. The values $\psi_x=k_xL$, $\psi_y=k_yL$ and $\psi_z=k_zL$ have the meaning of phase shifts per lattice period L. An integral equation (IE) is obtained by equating the left-hand side of Eq. (12) to zero at points belonging to the surface of wires. Under the assumption of thin wires $r_0 \ll L$, $r_0 \ll \lambda$, we neglect the azimuthal currents and the integral equation reduces to

$$\int_S G_{yy}(\mathbf{r},\mathbf{r}')J_y(\mathbf{r}')d\mathbf{r}' + \int_S G_{yz}(\mathbf{r},\mathbf{r}')J_z(\mathbf{r}')d\mathbf{r}' = 0, \quad \mathbf{r}\in S,$$

$$\int_S G_{zy}(\mathbf{r},\mathbf{r}')J_y(\mathbf{r}')d\mathbf{r}' + \int_S G_{zz}(\mathbf{r},\mathbf{r}')J_z(\mathbf{r}')d\mathbf{r}' = 0, \quad \mathbf{r}\in S. \tag{15}$$

A. Transformation of Green's function

We will use the Poisson summation rule

$$2\pi\sum_{m=-\infty}^{\infty}\varphi(2\pi m) = \sum_{m=-\infty}^{\infty}F[\varphi](m), \tag{16}$$

where

$$F[\varphi](m) = \int_{-\infty}^{\infty}\varphi(x)e^{imx}dx. \tag{17}$$

In our case

$$\varphi(2\pi m) = \sum_{n=-\infty}^{\infty}\sum_{l=-\infty}^{\infty}\frac{e^{-i[\beta_n\overline{y}+\gamma_l\overline{z}]}e^{-ik_x\overline{x}}e^{-i2\pi m\overline{x}/L}}{k_0^2\epsilon_h - (k_x+2\pi m/L)^2 - \beta_n^2 - \gamma_l^2}. \tag{18}$$

Denoting

$$S = -\frac{1}{V}\sum_{m=-\infty}^{\infty}\varphi(2\pi m), \tag{19}$$

where $V=L^3$, using Eq. (18) and the Poisson summation rule (16) we obtain

$$S = -\frac{1}{2\pi V}\times\sum_{n=-\infty}^{\infty}\sum_{l=-\infty}^{\infty}e^{-i[\beta_n\overline{y}+\gamma_l\overline{z}]}\sum_{m=-\infty}^{\infty}\int_{-\infty}^{\infty}\frac{e^{-ik_x\overline{x}}e^{-it\overline{x}/L}e^{imt}}{k_0^2\epsilon_h - (k_x+t/L)^2 - \beta_n^2 - \gamma_l^2}dt. \tag{20}$$

We introduce a new variable $\xi=k_x+t/L \rightarrow t=L(\xi-k_x)$; $dt=L\,d\xi$. The integrand (20) has poles at the points $\xi_{nl}=\sqrt{\beta_n^2+\gamma_l^2-k_0^2\epsilon_h}$. Calculating the integral by residuum method, we obtain

$$S = \frac{1}{2L^2}\sum_{n=-\infty}^{\infty}\sum_{l=-\infty}^{\infty}e^{-i[\beta_n\overline{y}+\gamma_l\overline{z}]}\sum_{m=-\infty}^{\infty}e^{-im\psi_x}\frac{e^{-t_{nl}|mL-\overline{x}|}}{t_{nl}}, \tag{21}$$

where $t_{nl}=\sqrt{\beta_n^2+\gamma_l^2-k_0^2\epsilon_h}$.

Let us present the sum of series as

$$S = S_0(m=0) + S_1(m\neq 0). \tag{22}$$

Here

$$S_0 = \frac{1}{2L^2}\sum_{n=-\infty}^{\infty}\sum_{l=-\infty}^{\infty}e^{-i[\beta_n\overline{y}+\gamma_l\overline{z}]}\frac{e^{-t_{nl}|\overline{x}|}}{t_{nl}}. \tag{23}$$

The series S_1 can be calculated at $\beta_n^2+\gamma_l^2 > k_0^2\epsilon_h$ using the geometrical progression formula. It results in

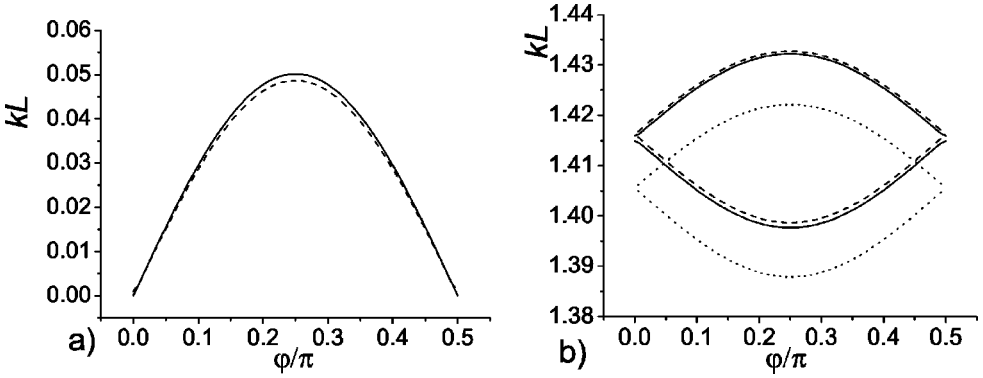

FIG. 3. Dispersion of low order propagating modes, calculated using electrodynamical and effective medium models in comparison with numerical results [7]. Normalized frequency for the propagating modes versus the angle φ. The solid curves correspond to our numerical results, the dashed curves correspond to the EM model, and the dotted curves show results [7] excluding the dispersionless mode. (a) shows the low frequency mode, and (b) shows the two modes above the plasma resonance.

$$S_1 = \frac{1}{2L^2} \sum_{n,l=-\infty,\beta_n^2+\gamma_l^2>k_0^2\epsilon_h}^{\infty} \frac{e^{-i(\beta_n\overline{y}+\gamma_l\overline{z})}}{t_{nl}} \times\left\{ \frac{e^{t_{nl}\overline{x}}e^{-i\psi_x-t_{nl}L}}{1-e^{-(i\psi_x+t_{nl}L)}} + \frac{e^{-t_{nl}\overline{x}}e^{+i\psi_x-t_{nl}L}}{1-e^{+i\psi_x-t_{nl}L}} \right\}. \quad (24)$$

In the case $\beta_n^2+\gamma_l^2<k_0^2\epsilon_h$ it is necessary to use the original expression (14) for calculation of $S_1(m\neq 0)$ with finite numbers of n and l.

B. Solution of the integral equation

Because the structure is homogeneous within periods in the y and z directions, it is natural to use exponential bases for the solution of the IE (12) by the method of moments (MOM), as in [7]. Let us expand the longitudinal currents into series of exponents:

$$J_y(y') = \sum_{j=0}^{M} a_j e^{i\beta_j y'}, \quad J_z(z') = \sum_{j=0}^{M} b_j e^{i\gamma_j z'}, \quad (25)$$

where $M+1$ is the number of basis functions in the expansion of the current. After application of the MOM to Eq. (12) the following system of equations is obtained:

$$\sum_{p=0}^{M} a_p G_{yy}^{sp} + \sum_{p=0}^{M} b_p G_{yz}^{sp} = 0 \quad (s=0,\ldots,M),$$

$$\sum_{p=0}^{M} a_p G_{zy}^{sp} + \sum_{p=0}^{M} b_p G_{zz}^{sp} = 0 \quad (s=0,\ldots,M). \quad (26)$$

Expressions for the matrix elements G_{yy}^{ps}, G_{yz}^{ps}, G_{zy}^{ps}, and G_{zz}^{ps} are given in the Appendix. The solution, which can be either k for fixed propagation constants k_x, k_y, k_z or one of k_σ, $\sigma=x, y, z$, under fixed k and other propagation constants, is found by equating the determinant of (26) to zero. Note that our method, which exploits the three-dimensional dyadic Green's function, is the full-wave one in contrast to the scalar local field approach [8], where instead of summation of the series responsible for the periodicity on the x axis, a sheet of average current was introduced.

IV. MODES IN THE *yz* PLANE

In this section extraordinary propagating and evanescent modes in the yz plane will be discussed, including complex waves. Results obtained using the effective medium approach and the numerical Green's function method are compared.

A. Propagating modes

Let us compare the known results obtained from numerical calculation and the effective medium approach. Figure 3 demonstrates the dispersion characteristics of a few lower propagating modes, calculated using the algorithm described above, the effective medium approach, and in comparison with the results of [7]. The parameters of the WM are taken the same as in [7]: the wire radius $r_0=0.01L$, where L is the lattice constant, and $\delta=L/2$ (Fig. 1). As in [7], we assume that the modulus of the wave vector is fixed, $q=0.1\pi/L$, and its components are $\mathbf{q}=q(0,\cos\varphi,\sin\varphi)$ (waves propagate in the yz plane). The plasma wave number used in the EM formula (10) was calculated according to the model [2], and it equals $k_pL\approx 1.38$ for this geometry (in [7] $k_pL\approx 1.37$ is used). Writing $k_y=q\cos\varphi$ and $k_z=q\sin\varphi$, the cubic equation (10) gives three different real solutions for k. These solutions are also seen in Fig. 2 at $\theta=\pi/2$. There are three extraordinary modes: One can propagate at very low frequencies, and two others a little above the plasma frequency. Good agreement between the results given by the Green's function method and the EM approach and a small difference (less than 1%) with [7] is observed. Figure 3 is separated into two parts in order to show the difference between the results of the EM and the full-wave solutions. This low frequency mode was missed by the authors of [7,8]. Thus we have shown that the EM model (11) is applicable both at low and at quite high frequencies above the plasma resonance.

B. Evanescent modes

Next, let us consider evanescent modes in the same medium, assuming $\mathbf{q}=q(0,i\cos\varphi,i\sin\varphi)$, $q=0.1\pi/L$. With the given parameter values the effective medium equation (10)

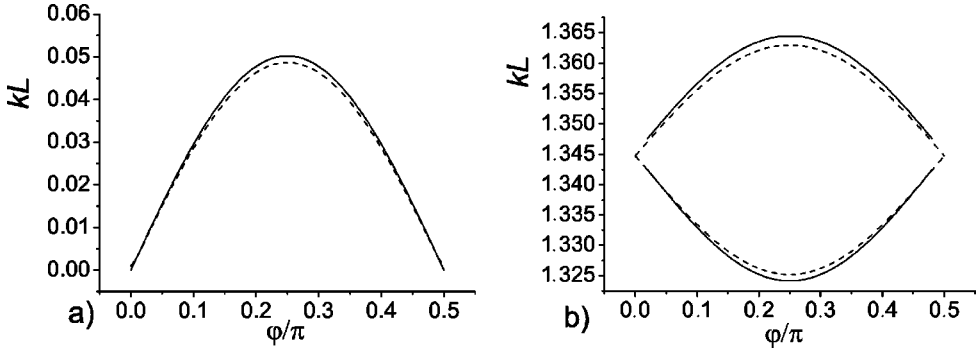

FIG. 4. Dispersion of evanescent modes, electrodynamical calculation (solid curves) and the EM theory (dashed curves).

gives three real solutions for k. Figures 4(a) and 4(b) present the results given by the effective medium and the full-wave theories. Two modes were found a little below the plasma resonance [see Fig. 4(b)] and the third one within the same spectral range, as the lowest propagating mode [compare Figs. 3(a) and 4(a)].

Further, in contrast with the discussion below, we fix the normalized frequency k and calculate the corresponding propagation constants k_z and k_y. Consider first the dispersion diagram k_z versus k_y for a fixed k. The effective medium theory gives four solutions, two for each propagation direction. Figure 5 illustrates such dependence, calculated at $kL=0.2\pi$ and using both EM and electrodynamical models. As was shown in [8], a mode can propagate at very low frequencies under conditions $k_y>k$, $k_x=0$; see Fig. 5, the curve marked by $k'_{z1}[k'_{z1}=|\mathrm{Re}(k_{z1})|, \mathrm{Im}(k_{z1})=0]$. Since this solution is a real one, the corresponding hyperbolic-type dispersion line can be called the isofrequency. At the same time, the second solution, shown by the curve $k''_{z2}[k''_{z2}=\mathrm{Im}(k_{z2}), \mathrm{Re}(k_{z2})=0]$, is purely imaginary at $k_y>k$.

At $k_y<k$ there are four complex solutions:

$$k_{z1} = k'_z + ik''_z,$$

$$k_{z2} = -k'_z + ik''_z,$$

$$k_{z3} = k'_z - ik''_z,$$

$$k_{z4} = -k'_z - ik''_z, \tag{27}$$

where $k'_z=|\mathrm{Re}(k_z)|$, $k''_z=|\mathrm{Im}(k_z)|$. The real and imaginary parts of k_{z1} are shown in Fig. 5. It is remarkable that the EM theory results coincide with a high accuracy with the results of the numerical simulation. It means that these peculiarities of the wave process in a 2D WM can be described by the macroscopic model of an effective spatially dispersive medium. If we consider the eigenvalue problem, these four solutions are independent, but physically such solutions are unacceptable because the amplitude of the Poynting vector will increase or decrease along the propagation direction, which is impossible in a lossless medium. However, if we combine the solution (27) in the form of standing waves with complex amplitudes

$$E_1(z) = e_1 e^{-k''_z z}\cos k'_z z,$$

$$E_2(z) = e_2 e^{-k''_z z}\sin k'_z z,$$

$$E_3(z) = e_3 e^{k''_z z}\cos k'_z z,$$

$$E_4(z) = e_4 e^{k''_z z}\sin k'_z z, \tag{28}$$

this difficulty disappears because the time averaged Poynting vector is zero at any z. That is why the basis (28) is more appropriate than the exponential one at least for solution of problems of wave reflection from an interface of a 2D WM. These solutions suggest the possibility for existence of localized electromagnetic fields near inhomogeneities.

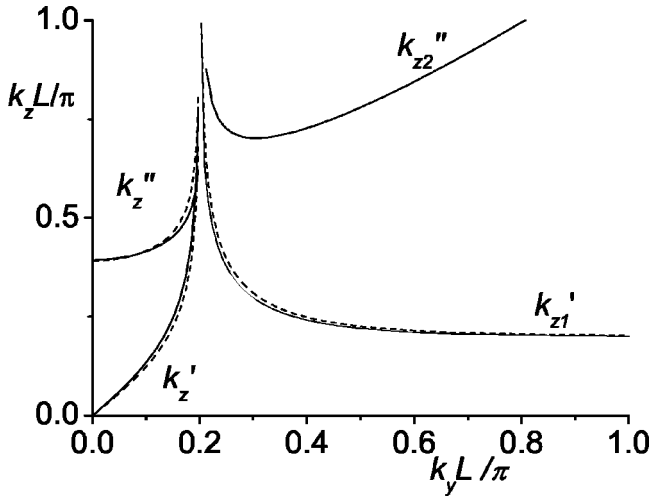

FIG. 5. Dispersion diagram k_z versus k_y. The real and imaginary parts of k_z calculated using the electrodynamical model (solid curves) and the EM theory (dashed curves).

C. Propagation in the z direction

Next, let us consider an important case when k and k_y are fixed and we have to determine the corresponding k_z. Let k_y be real. Such a problem is necessary to consider when we solve the problem of wave reflection from a medium interface, i.e., $k_y=k\sin\theta$, where θ is the incidence angle. Although the waves can propagate in a 2D WM even at very low frequencies, we always have the case $k_y<k$ and fall into

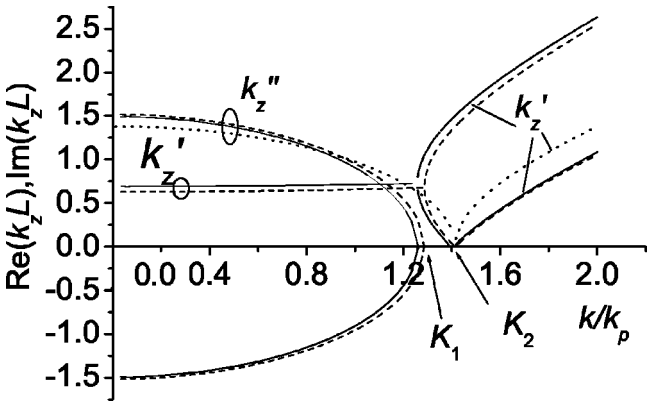

FIG. 6. Real and imaginary parts of k_z, calculated using the electrodynamical model (solid curves) and the EM theory (dashed curves). The dotted curve shows k_z given by the conventional plasma model.

the region of complex solutions for k_z ($\epsilon_h=1$ is assumed). Two waves propagating or attenuating in both directions follow from the EM theory (11). The conventional isotropic plasma model leads to only one wave for a certain direction, namely, $k_z=\sqrt{k_0^2\epsilon-k_y^2}$, $\epsilon=\epsilon_h(1-k_p^2/k_0^2\epsilon_h)$.

Real and imaginary parts of k_z versus the normalized frequency k/k_p are presented in Fig. 6 for $\theta=\pi/4$. In the simple case of the conventional model (dotted curve) k_z is imaginary if $k<K_2=k_p/\cos\theta$, and it is real if $k>K_2$. ($\epsilon_h=1$ is assumed.) The solution of the conventional model is completely wrong between K_1 and K_2 because it gives an imaginary value of k_z instead of a real one, obtained from the correct model. The correct, more complicated solutions, follow from Eq. (11). Analyzing Eq. (11), one can see that there exist three frequency regions, corresponding to different kinds of solution.

The first one is the low frequency band $k<K_1$, where

$$K_1 = k_p \frac{\sqrt{2}}{\sin\theta}\sqrt{\frac{1-\cos\theta}{\cos\theta}}. \tag{29}$$

There the propagation constant k_z is complex despite the fact that we have assumed the medium to be lossless (see Fig. 6). Actually, there are two complex conjugate solutions for each $\mathrm{Re}(k_z)>0$. The complex waves in lossless media do not transfer energy and exist in stop bands of periodic structures [12], ferrite films [13], and other media.

The second frequency area is $K_1<k<K_2$. Here K_1 is the stop band edge: beyond this wave number the waves are propagating. At point K_2 one of the solutions is zero and within the range $K_1<k<K_2$ we have a forward wave and a backward wave with respect to the interface, which follows from the analysis of the isofrequencies, presented in Fig. 7 for the case $\theta=\pi/4$. It means that one of the waves has a positive projection of the wave vector on the interface inner normal, while the other wave has a negative projection. The propagation directions of the refracted waves can also be found from the isofrequencies. In both these waves the group velocity vector has a positive projection on the inner normal, and the refraction is positive. Similar isofrequencies are presented in [8]. In the cases $\theta=\pi/15$ and 0 both positive and negative refractions take place for different waves.

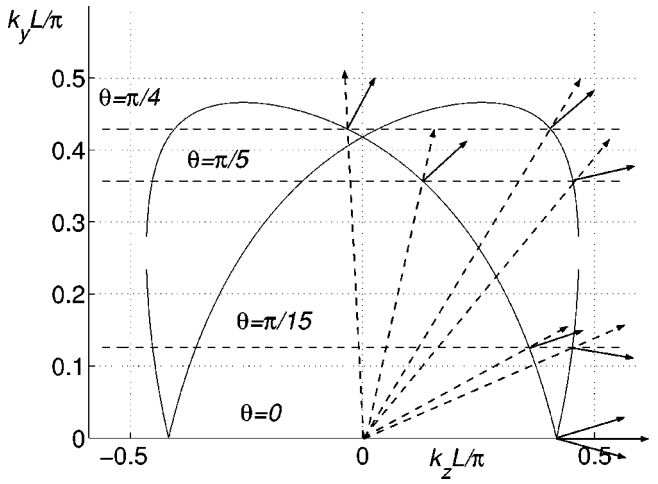

FIG. 7. Isofrequencies calculated at $k/k_p=1.35$ and their sections by the lines $k_y=k\sin\theta$ are shown for different θ. Dashed and solid arrows show directions of the phase and group velocities, respectively.

Finally, for $k>K_2$ both of the waves are propagating forward waves. Electrodynamical calculations confirm the results of the effective medium theory with a high accuracy in a wide spectral range including the regions of evanescent and propagating waves (see the solid and dashed curves in Fig. 6). Note that point K_2 corresponds to the edge of the passband in the framework of the old model. Thus, the model taking into account spatial dispersion leads to a considerably more complicated structure of eigenwaves than the conventional model of an isotropic plasma, and it is in very good agreement with the results of the full-wave analysis.

V. PROPAGATION ALONG THE *x* AXIS

We assumed above that the propagation constant k_x is equal to zero. In this section we consider the wave propagation along the x axis for the low frequency mode, shown by the bottom surface in Fig. 2. The results of detailed calculations of the propagation factor k_x using the EM and numerical models are presented in Fig. 8. Here the transverse wave vector lies on the diagonal of the lattice, i.e., $k_y=k_z$. The theory gives the formula

$$k_x^2 = k^2 - k_p^2 \pm \frac{k_y k_z k_p^2}{\sqrt{k^2-k_y^2}\sqrt{k^2-k_z^2}} - k_y^2 - k_z^2, \tag{30}$$

which is illustrated in Fig. 8 with dotted curves. Evidently, $k_x\to\infty$ if $k_y\to k$, $k_z\to k$ ($kL=0.4\pi$). The numerical results demonstrate a difference from the EM approach if $k_xL\to\pi$ and $k_y\to k$. It is explainable because in continuous media a propagation factor can go to infinity, but in periodic ones k_xL cannot exceed π for the fundamental spatial harmonic, and we observe higher order harmonics beyond π (see the solid lines). At this point both dispersion branches cross. Moreover, at this point $k_y=k$ and $k_z=k$. This is the frequency point at which two transmission-line modes appear propagating

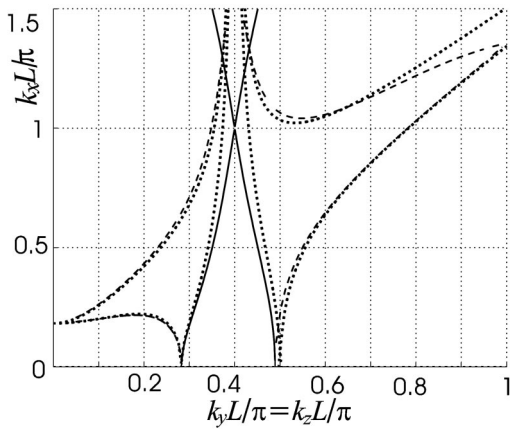

FIG. 8. Normalized propagation factor k_x versus normalized $k_y=k_z$, calculated for $kL=0.4\pi$. Solid and dashed lines show the real and imaginary parts of k_x, respectively, calculated using the MOM. Dotted lines illustrate the results obtained by the EM approach (both real and imaginary parts of k_x).

along *y* wires and along *z* wires, whereas the polarization of these modes is alternating from one set of wires to another (along the *x* axis). So the bisectorial in-plane propagation of the eigenwave is in fact the superposition of two independent waves. The EM theory, which loses the periodicity along the *x* axis, cannot catch this effect. This is why in the vicinity of this point the analytical curves disagree with the numerical ones.

Also evanescent waves (imaginary k_x) for real $k_y=k_z$ were considered. For the evanescent waves the results of the MOM and the EM theories are in quite good agreement, for low magnitudes of k_x especially (the results coincide with graphical precision for the wave having the smallest real k_y and imaginary k_x). A similar difference in k_x presented by higher order harmonics in the MOM model and in the EM model is observed at larger values of k_x. We can conclude that the EM theory is quite applicable for a 2D WM even if $k_x \neq 0$. Since for $k_x \neq 0$ the waves cannot be separated into ordinary and extraordinary ones, the effect of trirefrigence should take place under plane wave refraction on an interface of the 2D WM in the general case if one of the wire arrays is parallel to the interface.

VI. CONCLUSION

We have illustrated with additional examples that two-dimensional wire media should be described at low frequencies by a model that takes into account spatial dispersion, as is already known for conventional one-dimensional wire lattices. Otherwise, nonphysical effects can be obtained. Strong spatial dispersion causes physical effects like the appearance of anisotropy in lattices with square cells as well as the existence of an additional extraordinary wave. Propagating waves and evanescent waves with complex propagation constants have been studied using the effective medium approach and numerical simulations. The excellent agreement between the results given by both the models manifests that mainly effective medium "plasma" effects are responsible for the wave properties of 2D WMs.

Waves can propagate in a 2D WM at very low frequencies except in the propagation directions where the electric field vector is parallel to one of the wire arrays. Trirefrigence can be observed in the general case of plane wave refraction on an interface of a 2D WM if the interface is parallel to one of wire arrays. More refracted waves are obtained if the interface is tilted with respect to the wires. Possible applications of 2D WMs include antenna structures, low frequency filters, frequency selective radomes, and double negative metamaterials.

ACKNOWLEDGMENTS

This work has been coordinated by the "Metamorphose" Network of Excellence and partially funded by the Academy of Finland and TEKES through the Center-of-Excellence program.

APPENDIX

The matrix elements G_{yy}^{sp}, G_{yz}^{sp}, G_{zy}^{sp}, G_{zz}^{sp} are obtained after substitution of expansion (25) into IE (15), projection on to the respective functions, and double integrating over the surface of conductors *S*:

$$G_{yy}^{sp}=\oint_\Gamma dx\,dz\oint_\Gamma dx'dz'\int_0^L\int_0^L G_{yy}(\mathbf{r},\mathbf{r}')e^{-i\beta_s y+i\beta_p y'}dy\,dy',$$

$$G_{yz}^{sp}=\oint_\Gamma dx\,dz\oint_\Gamma dx'dy'\int_0^L\int_0^L G_{yz}(\mathbf{r},\mathbf{r}')e^{-i\beta_s y+i\gamma_p z'}dy\,dz',$$

$$G_{zy}^{sp}=\oint_\Gamma dx\,dy\oint_\Gamma dx'dz'\int_0^L\int_0^L G_{zy}(\mathbf{r},\mathbf{r}')e^{-i\gamma_s z+i\beta_p y'}dz\,dy',$$

$$G_{zz}^{sp}=\oint_\Gamma dx\,dy\oint_\Gamma dx'dy'\int_0^L\int_0^L G_{zz}(\mathbf{r},\mathbf{r}')e^{-i\gamma_s z+i\gamma_p z'}dz\,dz', \tag{A1}$$

where Γ is the contour the around the wire. Let us consider the contour integrals

$$U_y^{nl}=\oint_\Gamma e^{-t_{nl}|x-x'|}e^{-i\beta_n(y-y')}\begin{Bmatrix} dx\,dy \\ dx'dy' \end{Bmatrix} \tag{A2}$$

and

$$U_z^{nl}=\oint_\Gamma e^{-t_{nl}|x-x'|}e^{-i\gamma_l(z-z')}\begin{Bmatrix} dx\,dz \\ dx'dz' \end{Bmatrix}. \tag{A3}$$

Expressing $x=r_0\cos\phi$, $y=r_0\sin\phi$, $z=r_0\sin\phi$, $x'=r_0\cos\phi'$, $y'=r_0\sin\phi'$, and $z'=r_0\sin\phi'$, the contour integrals can be evaluated:

$$U_{y,z}^{nl}=2\pi r_0 I_0(\sqrt{C_{y,z}^{nl}-iD_{y,z}^{nl}}) \tag{A4}$$

where $I_0(x)$ is the zero order modified Bessel function,

$$C_{y,z}^{nl} = r_0^2[(t'_{nl})^2 + (k''_{y,z})^2 - (t''_{nl})^2 - (k'_{y,z} + q_{n,l})^2],$$

$$D_{y,z}^{nl} = 2r_0^2[t'_{nl}t''_{nl} + k''_{y,z}(k'_{y,z} + q_{n,l})], \tag{A5}$$

$q_{n,l}=2\pi(n,l)/L$, $t'_{nl}=\mathrm{Re}(t_{nl})$, $t''_{nl}=\mathrm{Im}(t_{nl})$, $k'_{y,z}=\mathrm{Re}(k_{y,z})$, and $k''_{y,z}=\mathrm{Im}(k_{y,z})$. According to formulas (A5), the sign of the exponent index does not matter. Then

$$G_{yy}^{sp} = \begin{cases} \dfrac{\delta_{sp}(\beta_s^2 - k_0^2\epsilon_h)}{2} \displaystyle\sum_{l=-\infty}^{\infty} \left[1 + \frac{e^{-i\psi_x - t_{sl}L}}{1 - e^{-i\psi_x - t_{sl}L}} + \frac{e^{i\psi_x - t_{sl}L}}{1 - e^{i\psi_x - t_{sl}L}}\right] \dfrac{(U_z^{sl})^2}{t_{sl}}, & \beta_s^2 + \gamma_l^2 > k_0^2\epsilon_h, \\ -\dfrac{\delta_{sp}(\beta_s^2 - k_0^2\epsilon_h)}{L} \displaystyle\sum_{m=-\infty}^{\infty} \sum_{l} \frac{(V_z^{ml})^2}{g_{msl}}, & \beta_s^2 + \gamma_l^2 < k_0^2\epsilon_h, \end{cases} \tag{A6}$$

where δ_{sp} is the Kronecker symbol and

$$V_z^{ml} = \oint_\Gamma e^{-i[\alpha_m(x-x') + \gamma_l(z-z')]} \begin{Bmatrix} dx\,dz \\ dx'dz' \end{Bmatrix} = 2\pi r_0 I_0(\sqrt{E_z^{ml} - iF_z^{ml}}), \tag{A7}$$

where $I_0(x)$ is the zero order modified Bessel function and

$$E_z^{ml} = r_0^2[(k''_z)^2 - \alpha_m^2 - (k'_z + q_l)^2],$$

$$F_z^{ml} = 2r_0^2 k''_z(k'_z + q_l). \tag{A8}$$

The next matrix elements are equal to

$$G_{yz}^{sp} = \begin{cases} \dfrac{\beta_s\gamma_p}{2}\left[1 + \dfrac{e^{-i\psi_x - t_{sp}L}}{1 - e^{-i\psi_x - t_{sp}L}} + \dfrac{e^{i\psi_x - t_{sp}L}}{1 - e^{i\psi_x - t_{sp}L}}\right] \dfrac{U_z^{sp}U_y^{sp}}{t_{sp}} e^{-t_{sp}\delta}, & \beta_s^2 + \gamma_p^2 > k_0^2\epsilon_h, \\ -\dfrac{\beta_s\gamma_p}{L} \displaystyle\sum_{m=-\infty}^{\infty} \frac{V_z^{ms}V_y^{mp}}{g_{msp}} e^{-i\alpha_m\delta}, & \beta_s^2 + \gamma_p^2 < k_0^2\epsilon_h, \end{cases} \tag{A9}$$

where

$$V_y^{mn} = \oint_\Gamma e^{-i[\alpha_m(x-x') + \beta_n(y-y')]} \begin{Bmatrix} dx\,dy \\ dx'dy' \end{Bmatrix} = 2\pi r_0 I_0(\sqrt{E_y^{mn} - iF_y^{mn}}), \tag{A10}$$

$$E_y^{mn} = r_0^2[(k''_y)^2 - \alpha_m^2 - (k'_y + q_n)^2],$$

$$F_y^{mn} = 2r_0^2 k''_y(k'_y + q_n), \tag{A11}$$

and

$$G_{zy}^{sp} = \begin{cases} \dfrac{\beta_p\gamma_s}{2}\left[1 + \dfrac{e^{-i\psi_x - t_{ps}L}}{1 - e^{-i\psi_x - t_{ps}L}} + \dfrac{e^{i\psi_x - t_{ps}L}}{1 - e^{i\psi_x - t_{ps}L}}\right] \dfrac{U_z^{ps}U_y^{ps}}{t_{ps}} e^{-t_{ps}\delta}, & \beta_p^2 + \gamma_s^2 > k_0^2\epsilon_h, \\ -\dfrac{\beta_p\gamma_s}{L} \displaystyle\sum_{m=-\infty}^{\infty} \frac{V_z^{mp}V_y^{ms}}{g_{mps}} e^{i\alpha_m\delta}, & \beta_p^2 + \gamma_s^2 < k_0^2\epsilon_h. \end{cases} \tag{A12}$$

Finally,

$$G_{zz}^{sp} = \begin{cases} \dfrac{\delta_{sp}(\gamma_s^2 - k_0^2\epsilon_h)}{2} \displaystyle\sum_{n=-\infty}^{\infty} \left[1 + \frac{e^{-i\psi_x - t_{sn}L}}{1 - e^{-i\psi_x - t_{sn}L}} + \frac{e^{i\psi_x - t_{sn}L}}{1 - e^{i\psi_x - t_{sn}L}}\right] \dfrac{(U_y^{sn})^2}{t_{sn}}, & \beta_n^2 + \gamma_s^2 > k_0^2\epsilon_h, \\ -\dfrac{\delta_{sp}(\gamma_s^2 - k_0^2\epsilon_h)}{L} \displaystyle\sum_{m=-\infty}^{\infty} \sum_{n} \frac{(V_y^{mn})^2}{g_{mns}}, & \beta_n^2 + \gamma_s^2 < k_0^2\epsilon_h. \end{cases} \tag{A13}$$

Let us analyze convergence of the series in the matrix elements (A6), (A9), (A12), and (A13). First we note that U_z^{nl} decays as $1/\sqrt{n}$ or $1/\sqrt{l}$ if $n\to\infty$ or $l\to\infty$ due to the asymptotic behavior of the Bessel function. The same relates to the terms U_y^{nl}, V_z^{ml}, and V_y^{ml}. Then only the first series in square brackets of the elements G_{yy}^{sp} and G_{zz}^{sp} converge as $1/l^2$ or $1/n^2$. The series Σ_m under conditions like $\beta_s^2+\gamma_p^2<k_0^2\epsilon_h$ converge as $1/m^3$. Other series converge exponentially.

[1] J. Brown, Prog. Dielectr. **2**, 195 (1960).

[2] P. A. Belov, S. A. Tretyakov, and A. J. Viitanen, J. Electromagn. Waves Appl. **16**, 1153 (2002).

[3] P. A. Belov, R. Marques, S. I. Maslovski, I. S. Nefedov, M. Silveirinha, C. R. Simovski, and S. A. Tretyakov, Phys. Rev. B **67**, 113103 (2003).

[4] I. S. Nefedov and A. J. Viitanen, *Guided Waves in Uniaxial Wire Medium Slab*, Progress in Electromagnetic Research, PIER 51 (EMW Publishing, Cambridge, MA, 2005), pp. 167–185.

[5] J. B. Pendry, A. J. Holden, W. J. Stewart, and I. Youngs, Phys. Rev. Lett. **76**, 4773 (1996).

[6] D. F. Sievenpiper, M. E. Sickmiller, and E. Yablonovitch, Phys. Rev. Lett. **76**, 2480 (1996).

[7] M. G. Silveirinha and C. A. Fernandes, IEEE Trans. Microwave Theory Tech. **52**, 889 (2004).

[8] C. R. Simovski and P. A. Belov, Phys. Rev. E **70**, 046616 (2004).

[9] D. R. Smith, W. J. Padilla, D. C. Vier, S. C. Nemat-Nasser, and S. Schultz, Phys. Rev. Lett. **84**, 4184 (2000).

[10] S. Tretyakov, *Analytical Modeling in Applied Electromagnetics* (Artech House, Boston, 2003).

[11] I. S. Nefedov and A. J. Viitanen, in Proceedings of the 27th ESA Antenna Technology on Innovative Periodic Antennas: Electromagnetic Bandgap, Left-handed Materials, Fractal and Frequency Selective Surfaces, Santiago de Compostela, Spain, 9–11 March, 2004 (ESA Conference Bureau, Noordwijk, The Netherlands, 2004), pp. 265–271.

[12] R. A. Silin, *Periodic Waveguides* (Phasis, Moscow, 2002) (in Russian).

[13] V. N. Ivanov, N. P. Demchenko, I. S. Nefedov, R. A. Silin, and A. G. Schuchinsky, Izv. Vyssh. Uchebn. Zaved., Radiofiz. **32**, 764 (1989) (in Russian).